

Column performance of carbon nanotube packed bed for methylene blue and orange red dye removal from waste water

G K Gill¹, N M Mubarak^{2*}, S Nizamuddin³ H S Al-Salim¹, J N Sahu⁴

¹Department of Chemical and Petroleum Engineering, Faculty of Engineering, UCSI University, Kuala Lumpur-56000, Malaysia

²Department of Chemical Engineering, Faculty of Engineering and Science, Curtin University, 98009 Sarawak, Malaysia

³Department of Chemical engineering, Scholl of engineering RMIT University Melbourne, Australia 3001

⁴Petroleum and Chemical Engineering Programme Area, Faculty of Engineering, Institut Teknologi Brunei, Tungku Gadong, P.O. Box 2909, Brunei Darussalam

Email: mubarak.mujuwar@curtin.edu.my; mubarak.yaseen@gmail.com

Abstract: Environmental issues have always been a major issue among human kind for the past decades. As the time passes by, the technology field has grown and has helped a lot in order to reduce these environmental issues. Industries such as metal plating facilities, mining operations and batteries production are a few examples that involves in the environmental issues. Carbon nanotube is proven to possess excellent adsorption capacity for the removal of methylene blue and orange red dyes. The effect of process parameters such as pH and contact time was investigated. The results revealed that optimized conditions for the highest removal for methylene blue (MB) (97%) and orange red (94%) are at pH 10, CNTs dosage of 1 grams, and 15 minutes for each dyes removal respectively. The equilibrium adsorption data obtained was best fit to Freundlich model, while kinetic data can be characterized by the pseudo second-order rate kinetics.

1. Introduction

Water is an important factor for a wide range of activities. The main source of contamination in water bodies is waste water run-off. Various industries discharge effluents that contain pollutants, which must be removed before it is released to the environment [1, 2]. Industrialization, agriculture practices and ecology changes are impacting the condition of water resources [3, 4]. Industries such as paper, pulp mills, paint, pharmaceutical, cosmetics, photographic, textile, leather, food, plastics and printing use huge amounts of dyes every year [5-7]. Large number of organic, inorganic and biological pollutants including pesticides, fertilizers, heavy metals, dyes, microbes etc. has been identified as water contaminants out of which some have serious side effects and few are believed to be dangerous and carcinogenic [3, 8-11]. World Bank appraises that material coloring and treatment contribute up to 17-20 percent of total industrial water pollution. Various techniques are available for the removal of heavy metal and dyes such as coagulation, adsorption, oxidation, chemical precipitation, membrane filtration, solvent extraction, electrochemical treatment, liquid-liquid extraction, reverse osmosis, photocatalytic degradation [12-14]. Adsorption is considered the most effective because it offers flexibility in operation and design; it also has a reversible nature as adsorbents can be regenerated by suitable



desorption processes for multiple use [15, 16]. Since discovery of carbon nanotubes (CNTs) is a new member in the carbon family [17]. CNTs have attracted researchers' interest as a type of adsorbent and offer an attractive option for the removal of organic and inorganic contaminants from water [18-21]. In addition CNTs is used for adsorption because of its unique properties; chemical and physical properties, optoelectronic, semiconductor, electrical, mechanical, structural properties, large specific surface area and extremely high thermal conductivity [22-24]. Hence, CNTs is most promising candidate especially in the field of remediation of toxic heavy metals, dyes contaminated industrial waste water [25, 26].

In this research, the comparative study on the removal of methylene blue (MB) and orange -red using batch adsorption study. The effect of the process parameters such as pH, contact time was investigated. Furthermore the kinetic and isotherm studies for the removal of both dyes were discussed.

2. Materials and method

2.1 Raw Materials

Microwave assisted CNTs were obtained from our previous [27]. The dyes used in this research are methylene blue and orange red obtained from Merck. Preparation of stock solution

2.2 Preparation of Stock Solution

Analytical grade of methylene blue (MB) and orange- red standards which were obtained from Merck were used to prepare stock solutions containing 1000 mg/L MB and orange -red which were further diluted with distilled water to obtain the required concentrations. In this research, the initial concentration of both MB and orange red dyes were set to 2 mg/L and prepared stock solution was used to batch adsorption experiments

2.3 Adsorption Experiment

The batch adsorption experiment was carried out using prepared stock solution with 2mg/L of both initial dyes concentration. The lower and upper values of each parameter (pH, and contact time) were chosen based on previous study on the removal of MB and orange red. The effect of process parameters such as pH (2 to 11) and contact time (10-50) using single factor optimization. The height of bed height was fixed 2cm (1 gram of CNTs). The experiments were carried out at constant room temperature. The pH values of the dye stock solutions were altered by using either 1.0 M of hydrochloric acid or 1.0 M of sodium hydroxide, depending on the value of desired pH. For the removal of MB and orange-red with fixed height (2 cm) which is used in this research, its adsorption capacity at time t was determined by using (1). As for the adsorption equilibrium of the dye, it was determined based on (2).

$$q_t = \frac{(C_o - C_t)V}{m} \quad (1)$$

$$q_e = \frac{(C_o - C_e)V}{m} \quad (2)$$

Where C_o represents the initial concentration of the dye solution (mg/L), C_t is the concentration of dye solutions at time t (mg/L), C_e is the concentration of dye at equilibrium, V is the volume of dye solution (L) and m is the weight of magnetic biochar adsorbent used (g).

2.4 Characterization of Dye Removal

The physical properties, structure, and morphology of microwave assisted CNTs were reported earlier. Fourier transform infrared (FTIR) spectroscope (Bruker, USA) was used to analyse the before and

after adsorption of dye on the surface of CNTs for the determination of the surface functional groups. All pH measurements were carried out using Mettler Toledo type (MP220 model, USA). The removal of dyes concentrations were measured by using the UV-Vis Spectro (U-29010 double beam, Perkin Elmer)

3. Results and discussion

3.1.1. Effect of pH on removal of MB and orange red

The pH factor is an important factor for the uptake of MB and orange red because the pH of a medium manipulates the magnitude of the electrostatic charges which are imparted by the ionized dye molecules [28, 29]. The pH factor causes the chemical characteristics of both adsorbent and adsorbate [30]. Hence, the rate of adsorption varies greatly in different mediums with different pH values. Fig 1(a-b) shows the effect of pH on removal of MB and orange-red respectively. From the observation as pH increase from pH2 to pH 10 increasing rapidly for both dye removal [31]. This is due to the pH increases, the number of H^+ ions decreases, therefore making the process more favourable. Further increase in pH 11 decrease in removal of both dyes was observed probably due to the presence of excess of OH ions competing with the dye anions for the adsorption sites [32-34]. In addition, an increase in pH will cause the density of the surface charge to decrease and this causes a lowering in the electrostatic repulsion between the surface of the CNT and the charge of MB and orange-red therefore the rate of adsorption increases. [35, 36]. Hence pH plays a vital role in adsorption of dye removal.

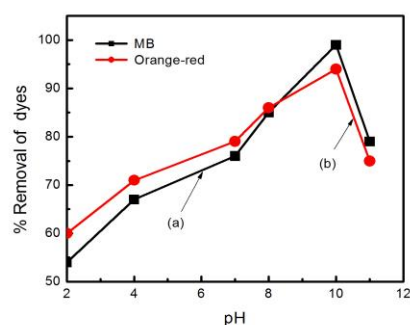


Figure 1. Effect of pH on (a) MB and (b) orange-red removal

3.2 Effect of contact time on MB and Organe-red

Figure 2 (a-b) shows the effect of contact time on removal of MB and orange-G respectively. It was observed as contact time increases from 10 min to 15 min rapid increase in removal of MB (99%) and orange-G (94 %) was observed. This is due to adsorption sites are vacant initially and the concentration gradient of solute is very high at the beginning of contact time. Further increase the contact time decreases percentage of removal of dyes was observed. The initial rapid rate of adsorption may be due to the availability of the positively charged surface of the adsorbent for anionic MB and orange-red species present in the solution. Occupation of the remaining vacant sites did not take place due to the high repulsive forces between the molecules of the dye at the adsorbent surfaces and in the bulk solution [37].

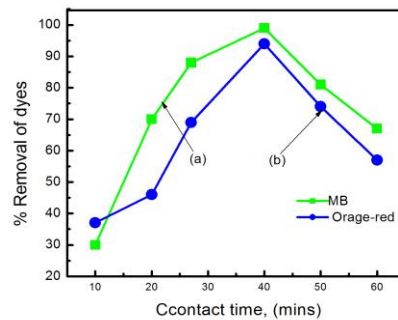


Figure 2. Effect of contact time on MB and orange-red removal.

3.3 Adsorption kinetic studies of MB and orange-red

The experiments for kinetic study were carried out for 2h minutes where three different pH values and initial concentration of the dye stock solution were used for the runs. From these three different beakers with different pH values of pH 4, pH 7 and pH 10 with initial concentration of 2 mg/L of MB and orange red respectively. The dye solution was measured every 5 minutes where later on the concentration at that specific time was checked by using the UV-Vis Spectrophotometer. Figures 3(a) and 3(b) are graphs of amount of dye adsorbed at time t , q_t against the contact time for MB and orange-red respectively. Adsorption of high initial concentration (2mg/L) results in an increase in the adsorption uptake due to increase in driving force leading to higher adsorption rate [14]. From the observation the rapid equilibrium was reached both dyes at 15 minutes and completed equilibrium was reached at 60 minutes. No significant additional adsorption was observed after 60 minutes. The contact time was thus maintained for 2 hr to ensure that the equilibrium could be achieved. These results was good agreement with others researchers [13, 31].

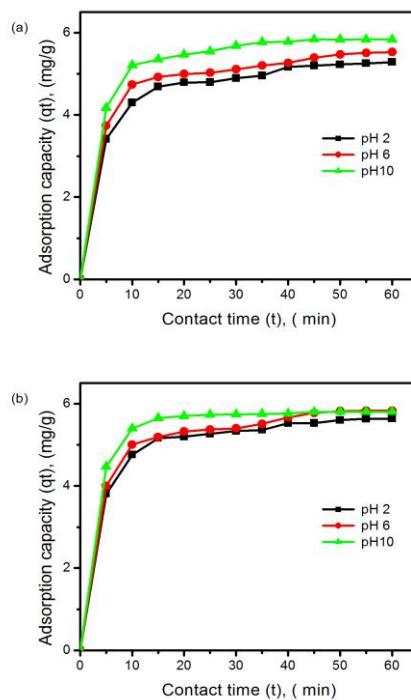


Figure 3 (a-b). The effect of contact time on adsorption capacity (a) MB, (b) orange-red

3.3.1 Adsorption kinetic study of MB and orange-red

In this research, the equilibrium data for the adsorption of the two dyes with varying concentrations of were fitted to two important equations; Langmuir equation and the Freundlich equation. The Langmuir isotherm could give a good relation between the solid phase concentration at equilibrium, q_e and equilibrium concentration of the dye solution, C_e , as shown in (3).

$$\frac{C_e}{q_e} = \frac{1}{k_L q_m} + \frac{C_e}{q_m} \quad (3)$$

Where C_e (mg/L) is the equilibrium concentration of dye solution, q_e is the amount of dye adsorbed at equilibrium (mg/g), K_L is the adsorption equilibrium constant (L/mg) and q_m is a constant and it reflects a complete monolayer (mg/g). K_L is a constant which links the affinity of the binding sites and q_m represents the maximum adsorption capacity of the magnetic biochar as adsorbent.

Fig. 4(a-b) are the linearized Langmuir models of C_e/q_e against C_e for isotherm studies for the removal of methylene blue and orange red dyes respectively. From these two figures, the values of K_L and q_m can be obtained. According to Fig. 4, the calculated value of q_m was found to be 45.66 mg/g and K_L to have a value of 0.17755 L/mg and for Fig. 4(b), the q_m value was calculated to be 31.26 mg/g and K_L is 0.384 L/mg. The Langmuir isotherm produces good fits over the range of concentration for the removal of these two dye solutions with R^2 values of 0.89 and 0.98 for methylene blue and orange red respectively. Another model of equation to be studied is the Freundlich model. Equation (4) shows the Freundlich equation for heterogeneous surface energy systems.

$$\ln q_e = \ln K_F + \frac{1}{n} \ln C_e \quad (4)$$

Where K_F and n are both the Freundlich constants that will be determined from the plot of $\ln q_e$ against $\ln C_e$. K_F and $1/n$ are interrelated to both the sorption capacity as well as the intensity of the sorption of the system. Besides, from the magnitude of the $1/n$ term, one can determine the favourability of the sorbent/adsorbate systems [8]. Fig. 5(a-b) are plots of the Freundlich adsorption isotherm for the removal of methylene blue and orange red dyes respectively. From observation it is found that the relationships between the uptake of dyes, q_e (mg/g) and the residual dye equilibrium concentration, C_e (mg/L) based on (6) were shown. Figure 5(a), the value of n is 1.462 and K_F to have a value of 7.422 (mg/g) (mg/L)^{1/n} and the R^2 value is 0.9310. As for the removal of orange red based on Fig.5 (b), the K_F value is 1.462 (mg/g) (mg/L)^{1/n} and n is 1.83. The R^2 value for the removal of this dye was found to be 0.96 and 0.989 for MB and orange red. Table 1 shows isotherm constant for both Langmuir and Freundlich isotherm.

Table 1. Isotherm parameters for dyes removal

Adsorbent	Langmuir Isotherm			Freundlich Isotherm		
	qm (mg/g)	KL (L/mg)	R ²	n	KF (L/mg)	R ²
MB	45.66	0.1775	0.8996	1.462	7.4224	0.9653
Orange-red	31.26	0.3844	0.98	1.832	9.148	0.998

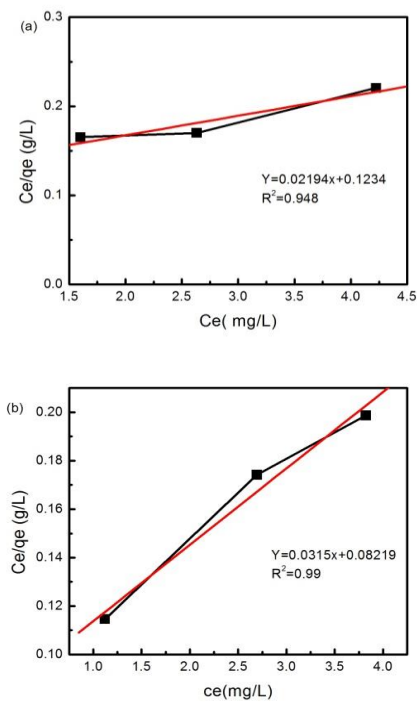


Figure 4. a) Langmuir adsorption MB and b) orange- red

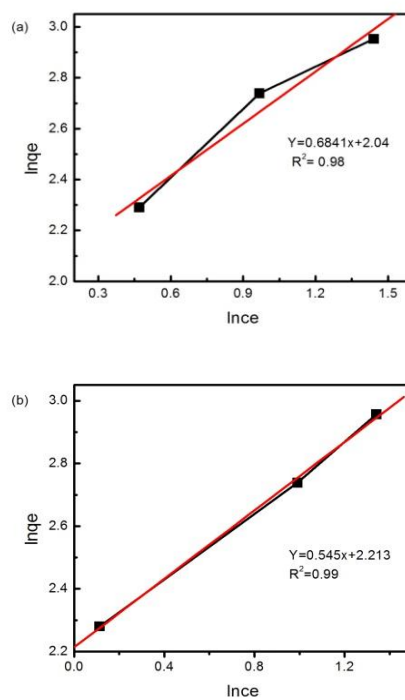


Figure 5. a) Freundlich isotherm MB b) orange- red.

The kinetic studies for the pseudo-first order and pseudo-second order were also carried out in this research. The purpose of carrying out this study is to develop a better understanding on the dynamics

of adsorption process. The linearized equations 5 and 6 are both used to study the pseudo-first order and second order models respectively.

$$\log(q_e - q_t) = \log q_e - \left(\frac{k_1}{2.303}\right)t \quad (5)$$

$$\frac{t}{q_t} = \frac{1}{K_2 \cdot q_e^2} + \frac{1}{q_e} \quad (6)$$

where q_e represents the amount of dye being adsorbed onto the adsorbent at equilibrium (mg/g), q_t represents the amount of dye being adsorbed onto the adsorbent at time t (mg/g), K_1 (min^{-1}) is the rate constant for pseudo-first order adsorption and K_2 ($\text{g mg}^{-1} \text{min}^{-1}$) represents the rate constant for the pseudo-second order adsorption. Besides that, according to the calculated values on Tables 2 and 3, the obtained R^2 values for pseudo-second order that are approaching unity are way higher than that of pseudo-first order. Also, the values of q_e and K_2 for pseudo-second order are proven to be consistent with the pH values

Table 2. Pseudo-first-order and pseudo-second-order kinetics for adsorption of MB and orange red

pH	MB			Orange Red		
	q_e (mg/g)	K_1 (min^{-1})	R^2	q_e (mg/g)	K_1 (min^{-1})	R^2
2	41.5	0.0001	0.7006	27.48	0.0001	0.851
6	41.21	0.0001	0.7216	27.98	0.0001	0.794
10	40.65	0.0606	0.5574	28.22	0.0001	0.896

Table 3. Pseudo-second-order kinetics for adsorption of MB and orange red

pH	MB			Orange red		
	q_e (mg/g)	K_2 (g/mg min)	R^2	q_e (mg/g)	K_2 (g/mg min)	R^2
2	5.48	0.0180	0.998	5.82	0.0246	0.999
6	5.71	0.0183	0.998	5.31	0.0264	0.999
10	5.96	0.0311	0.999	5.12	0.0223	0.999

3.4. Characterization of dyes Removal

3.4.1 FTIR analysis of dyes

Figure 6 (a-c) shows the FTIR image for the surface functional group of the raw CNT, MB and orange-red. The results indicate that the functional groups have been successfully impregnated on the surface of the adsorbent. The main bonds that represent the vibration of functional groups on the surface of CNTs. Figure 6 (a) shows less functional on the surface of CNTs was observed after adsorption of MB and orange-red as shown in figures 6(b-c). The peak at approximately 3500 cm^{-1} , shows characteristic of an H bonded O-H stretch on the CNT. Peak at $700\text{-}610 \text{ cm}^{-1}$ represents alkynes group with $-\text{C}\equiv\text{C}-\text{H}$: C-H bond in CNT. A sharp peak at approximately $1600\text{-}1750 \text{ cm}^{-1}$ corresponding to $\text{C}=\text{O}$ stretching vibration of the carboxylic acid on the CNT. A strong

peak appears at 2850 and 3000 cm^{-1} due to the C–H stretching in the adsorbent. The spectra of both dyes displays all characteristic peaks of the bonds in dyes, namely 1150 cm^{-1} due to C–H stretching vibrations in aromatic ring, 1650 cm^{-1} due to C=C stretching vibrations in aromatic nuclei, 2900 cm^{-1} due to C–H stretching vibrations of the crystal violet and a broad peak at 3400 cm^{-1} due to the presence of O–H bonds of the water molecules adsorbed on both dyes. The spectra of Copper metal display the peaks of bonds, 3200–3500 cm^{-1} O–H stretch, 1680–1640 cm^{-1} –C=C– stretch for alkenes functional group and C-H bond at 900–675 cm^{-1} having aromatic functional group. These results was good agreement with other researchers [29, 38].

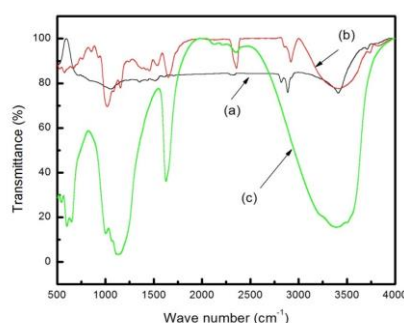


Figure 6. FTIR Images of a) Raw CNTs, b) MB C) orange –red

3.4.2 FESEM Analysis of dye

The CNT used for this research were analysed by using the Field Emission Scanning Electron Microscopy (FESEM) where Figure 7 (a-b) shows the morphology of the CNT. Figure 7 (a) shows the raw image of CNT before adsorption whereas Figure 7(b) shows after adsorption of dyes onto CNT with magnification scale of 1 μm . As it can be observed from Figure 7 (a), it is clearly shown that the surface texture of this raw CNT has a rather smooth surface and few pores can be seen on the surface. Figure 7 (b) shows the tubes after adsorption they open up as some functional groups on the surface of CNTs during adsorption therefore the surface is less smooth compared with the raw CNT. Similar observation was observed in previous researchers [39, 40]

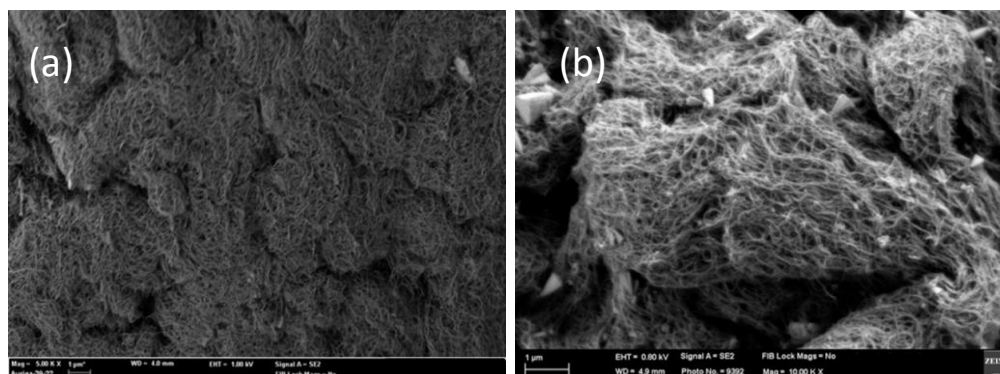


Figure 7. FESEM images of (a) raw CNT and (b) CNT after adsorption from dye.

4. Conclusion

Carbon nanotube is proven to possess excellent adsorption capacity for the removal of MB and orange red dyes. The process parameters for the maximum adsorption of MB and orange red dyes were pH 10, adsorbent dosage of 1.00 gram, and contact time of 15 minutes respectively. The equilibrium data for this research fitted very well in both Langmuir and Freundlich isotherms but was best described by the Langmuir model with a maximum adsorption capacity of 45.66 mg/g for methylene blue and 31.6 mg/g for MB and orange red respectively. As for the order of the reaction, the rates of adsorption for both dyes were found to comply with the pseudo-second order kinetic model.

References

- [1] Arzani K, Ashtiani B G and Kashi A H A 2012 *无机材料学报* **12050**
- [2] Muyibi S A, Ambali A R and Eissa G S 2008 *Water Policy* **10** pp193-206
- [3] Kumar S, Bhanjana G, Dilbaghi N and Umar A 2014 *J. Nanosci. Nanotechnol.* **14** pp7054-7059
- [4] Wang S, Boyjoo Y, Choueib A and Zhu Z H 2005 *Water Res.* **39** pp129-138
- [5] Aysu T and Küçük M 2015 *Int. J. Environ. Sci. Technol.* **12** pp2273-2284
- [6] Namasivayam C and Arasi D J S E 1997 *Chemosphere* **34** pp401-417
- [7] Namasivayam C, Yamuna R T and Arasi D J S E 2002 *Sci. Technol. Sep.* **37** pp2421-2431
- [8] Mubarak N, Sahu J, Abdullah E and Jayakumar N 2014 *Sep. Purif. Rev.* **43** pp311
- [9] Ruthiraan M, Mubarak N M, Thines R K, Abdullah E C, Sahu J N and Jayakumar N S 2015 *Korean J. Chem. Eng.* **32** pp446-457
- [10] Dehghani MH, Mostofi M, Alimohammadi M, McKay G, Yetilmezsoy K, Albadarin AB 2016 *J Ind Eng Chem* **35** pp63-74.
- [11] Mubarak NM, Fo YT, Al-Salim HS, Sahu JN, Abdullah EC, Nizamuddin S 2015 *Int J Nano* **14** 1550009.
- [12] Kant R 2012 *Natural science* **4** 22.
- [13] Madrakian T, Afkhami A, Ahmadi M and Bagheri H 2011 *J. Hazard. Mater.* **196** pp109-114
- [14] Gong J-L, Wang B, Zeng G-M, Yang C-P, Niu C-G and Niu Q-Y 2009 *J. Hazard. Mater.* **164** pp1517
- [15] Shahryari Z, Goharrizi A S and Azadi M 2010
- [16] Sabna V, Thampi SG and Chandrakaran S 2015 *Ecotoxicol Environ. Saf.*
- [17] Iijima S 1991 *Nature* **354** pp56-58
- [18] Dehghani M H, Mostofi M, Alimohammadi M, McKay G, Yetilmezsoy K and Albadarin AB 2016 *J. Ind. Eng. Chem.* **35** pp63-74.
- [19] Onundi Y B, Mamun A, Al Khatib M, Al Saadi M, Suleyman A. 2011 *Int. J. Env. Sci. Technol.* **8** pp799-806
- [20] AlSaadi M A, Al Mamun A, Alam M Z, Amosa M K and Atieh M A 2016 *Nano* **11** 1650011
- [21] Yu J-G, Zhao X-H, Yang H, Chen X-H, Yang Q and Yu L-Y 2014 *Sci. Total Environ.* **482** pp241-251
- [22] Ajayan P M 1999 *Chem. Rev.* **99** pp1787
- [23] Terrones M 2003 *Annual Rev. Mater. Res.* **33** pp419
- [24] Dai L and Mau A W H 2001 *Adv. Mater.* **13** pp899
- [25] Rao GP, Lu C and Su F 2007 *Sep. Purif. Technol.* **58** pp224
- [26] Yit Thai O, Abdul Latif A, Sharif Hussein Sharif Z and Soon Huat T 2010 *Brazilian J. Chem. Eng.* **27**
- [27] Mubarak N, Sahu J, Abdullah E, Jayakumar N and Ganesan P 2014 *Diam. Relat. Mater.* **48** pp52-59
- [28] Tabrizi N and Yavari M 2015 *Chem. Eng. Res. Des.* **94** pp516-523
- [29] Ghaedi M, Hajati S, Zaree M, Shajaripour Y, Asfaram A and Purkait M 2015 *Adv. Powder Technol.* **26** pp1087-1093
- [30] Yasin Y, Hussein M Z and Ahmad F H 2007 *The Malaysian J. Analyt. Sci.* **11** pp400-406
- [31] Ai L, Zhang C, Liao F, Wang Y, Li M and Meng L 2011 *J. Hazard. Mater.* **198** pp282-290
- [32] Wang S, Boyjoo Y, Choueib A and Zhu Z 2005 *Water Res.* **39** pp129
- [33] Ma J, Yu F, Zhou L, Jin L, Yang M and Luan J 2012 *ACS Appl. Mater. Interfaces* **4** pp5749-5760
- [34] Gupta V K, Kumar R, Nayak A, Saleh T A and Barakat M 2013 *Adv. Colloid Interface Sci.* **193** pp24-34
- [35] Gupta V and Nayak A 2012 *Chem. Eng. J.* **180** pp81-90
- [36] Ngah W W, Teong L and Hanafiah M 2011 *Carbohydr. Polym.* **83** pp1446-1456
- [37] Belay K and Hayelom A. 2014
- [38] Sadegh H, Shahryari-ghoshekandi R, Masjedi A, Mahmoodi Z and Kazemi M 2016 *Int J. Nano Dimension* **7** pp109-120

- [39] Păcurariu C, Paşka O, Ianoş R, Muntean SG 2016 *Clean Technologies and Environmental Policy* **18** pp705-715.
- [40] Yao Y, Bing H, Feifei X, Xiaofeng C 2011 *Chemical Engineering Journal* **170** pp82-89.